

Thermal performance of green roofs in dry climate regions of Mexico through simulation with energypius and openstudio Tools

ABSTRACT

Place and duration of Study: Faculty of Engineering, Universidad Autónoma de Querétaro, January 2022 to May 2023.

Green roofs are often used as an aesthetic resource by architecture, since they help to generate artificial green areas in densely populated urban areas, thanks to the fact that they occupy small spaces. This type of system has the quality that it also serves as a passive thermal insulation system. The majority of built green roofs are based on an extensive system, which is characterized by its low maintenance demand and low cost, as it has a shallow substrate and grass-based vegetation. However, in order to exploit the full potential of this system, the optimal parameters for each region must be studied, since the climatological characteristics of the place will directly affect its operation. Through the applied methodology, a base model configured in relation to a system previously established in the Autonomous University of Queretaro (UAQ) was obtained. With the model generated, the relationship between the thickness of the substrate and the decrease in internal temperature was studied, and differences of 5°C were obtained with respect to the external temperature.

Keywords: Green Roof, Thermal Comfort, Thermal Insulation, Green Energy. Computer Simulation

1. Introduction

Green roof systems are not something new, they have been around for several centuries, however, they were presented as rustic coverings used to protect the roof of houses as shown in Fig. 1. An example of these practices is It can be observed in Iceland, Canada and the United States. Where they were used as a barrier against the cold climate of the region [1].

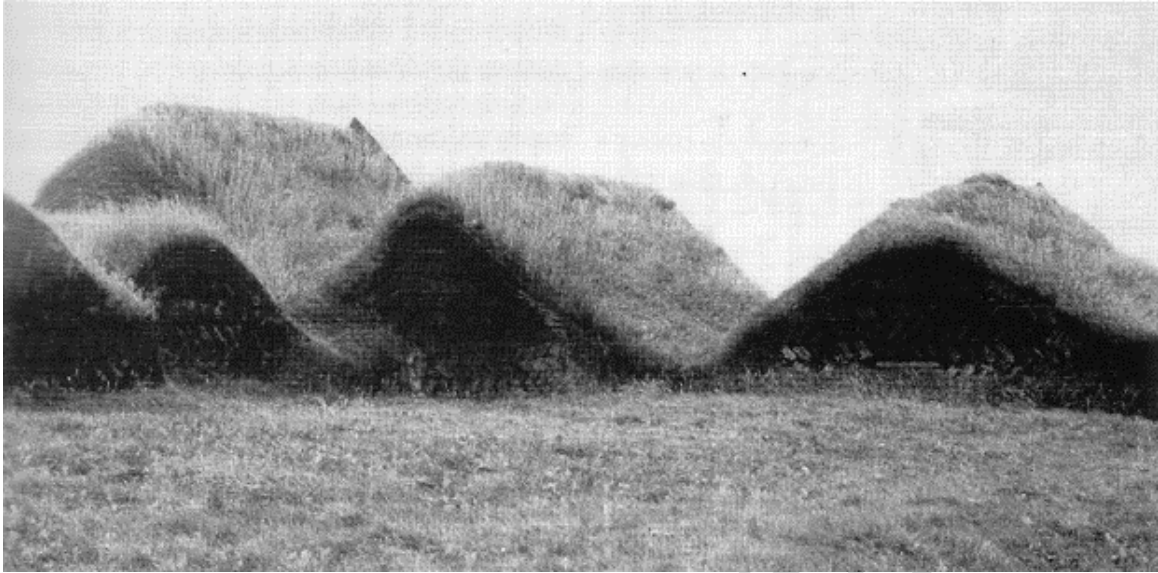


Figure 1 Traditional sod loaf houses (Iceland).

The green roof as we know it today emerged in Central Europe in the 1970s [2] and spread widely to the rest of the world at the beginning of the new millennium. At present there are thousands of covers that are covering the roofs of multiple buildings and homes [3].

Due to the increase in global temperature, the temperatures inside the houses have increased in the summer, resulting in a reduction in the thermal comfort of the occupants. What entails the increase in the consumption of electrical energy to feed air conditioners and other cooling systems [4,5]. In Mexico is observed that currently the energy demand of homes has increased more and more and represents 19.6% of the total demand of the country [6].

This demand for energy is also a consequence of the increase in the population in our country, which has followed an exponential trend in recent years, and although a decrease in the growth rate was observed in the last population census, the population continues to grow. and as a consequence, the number of necessary houses increases [6]. It is for this reason that the application of passive systems such as green roofs, would help to solve the energy demand to a certain extent.

Currently, green roofs can be divided into two groups: intensive and extensive; Intensive ones refer to roof gardens with shrubs and small trees that need a minimum substrate

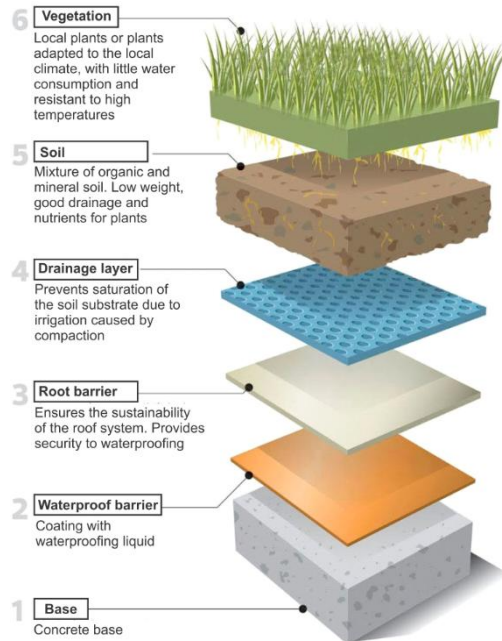


Figure 2 General scheme of green roof.

thickness of 30 cm, in contrast to extensive ones that are made up entirely of grasses generally and can develop in thicknesses of 10 to 30 cm [7]. . In Fig. 2 we can see a diagram of the different layers that make up an extensive green roof system.

If the green roof is taken into account as a part of the thermal envelope of a home or building, it will affect its energy consumption in terms of indoor temperature control, either to increase or decrease the temperature and achieve the thermal comfort of users [8]. In this same article it is shown that the results obtained will depend to a large extent on the thickness of the substrate layer and the percentage of moisture in it.

Even though several studies have been carried out to verify the qualities and characteristics of the green roof system in various climates [7,9], in some of these studies some variables have been left aside, as it is a complex system that requires a deep understanding of the relationships of the variables in each of its layers to be able to discern its behavior.

Some of these variables that directly influence the efficiency of the model that have been studied are: the thickness of the substrate layer, type of substrate [10]. However, other variables such as the construction of the drainage system, the optimal humidity to increase the heat transfer coefficient between the interior and exterior, to name a few.

Taking into account the aforementioned before being able to use the green roofs, a study should be carried out depending on the climate where the system is intended to be used: taking into account certain variables; such as the type of substrate to use, thickness of the substrate, optimal percentage of humidity to generate the greatest amount of heat transfer from the interior to the exterior in the summer season and the least in the winter season, always taking into account the minimum essential requirements for the survival of the

vegetal layer. It is for this reason that the behavior of the system is studied when humidity varies at certain times, an alternative irrigation system and the use of the drainage layer as a temporary water deposit.

2. Theoretical Background

The model used is known as “fastall-season soil strength” (FASST) developed by Frankenstein and Koenig for the United States Army and Engineering Corps [16,17].

In Fig. 3 the energy balance of a green roof is observed, it includes latent heat flux (L), sensible heat flux (H), short-wave radiation (Is), and incoming long-wave radiation (Iir), conduction in the ground and the complex exchange of long wave (LW) radiation within the foliage [11].

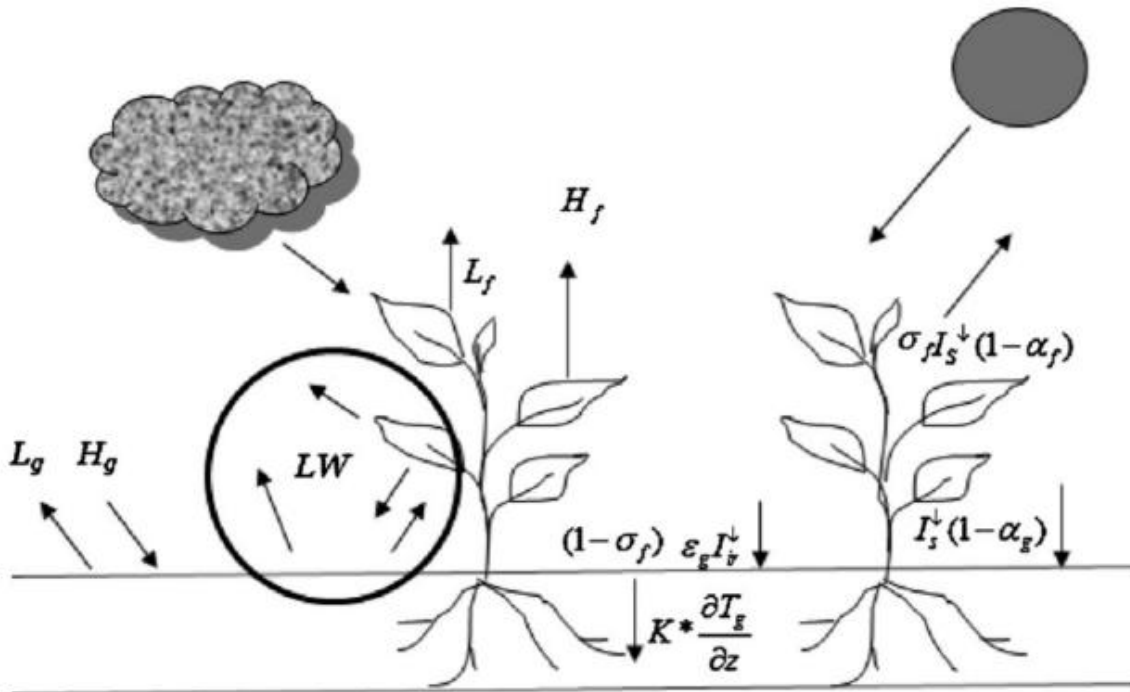


Figure 3 Energy balance of a green roof.

This energy analysis is divided into an analysis for the foliage layer (Ff) and an analysis for the soil surface (Fg). The numerous parameterizations used for the latent heat flux are described below in detail until reaching the simultaneous solution of two equations involving foliage temperature and soil surface.

Energy analysis for the foliage layer.

$$F_f = \sigma_f [I_s(1 - \alpha_f) + \epsilon_f I_{ir} - \epsilon_f \sigma T_f^4] + \frac{\sigma_f \epsilon_f \sigma}{\epsilon_1} (T_g^4 - T_f^4) + H_f + L_f \quad (1)$$

Where, F_f is the foliage layer, σ_f is the fractional vegetation coverage, I_s is the total incoming short-wave radiation, α_f is the albedo (short-wave reflectivity) of the canopy, ϵ_f is the emissivity of canopy, I_{ir} is the total incoming long-wave radiation, σ is the Stefan-Boltzmann constant ($5.67 \times 10^{-8} \text{ W/m}^2 \text{ K}^4$), T_g^4 is the ground surface temperature, T_f^4 is the

foliage temperature, $\varepsilon_1 = \varepsilon_g + \varepsilon_f - \varepsilon_f \varepsilon_g$, ε_g is the emissivity of the ground surface, H_f is the foliage sensible heat flux and L_f is the foliage latent heat flux.

In addition to convective and sensible heat transfer this equation accounts for both the short- and long-wave radiation absorbed by the vegetation, including the effects of multiple reflections.

Sensible heat flux in the foliage layer

$$H_f = (1.1LAI\rho_{af}C_{p,a}C_fW_{af})(T_{af} - T_f) \quad (2)$$

Where, LAI is the leaf area index, ρ_{af} is the density of air at foliage temperature, $C_{p,a}$ is the specific heat of air at constant pressure (1005.6 J-Kg K), C_f is the bulk heat transfer coefficient, W_{af} is the wind speed with in the canopy, T_{af} is the air temperature with in the canopy and T_f is the foliage temperature [18].

$$\rho_{af} = 0.5(\rho_a + \rho_f) \quad (3)$$

Where, ρ_{af} is the density of air at foliage temperature, ρ_a is the density of air at instrument height and ρ_f is the density of air at foliage temperature [19].

$$T_{af} = (1 - \sigma_f)(T_a) + \sigma_f(0.37T_a + 0.6T_f + 0.1T_g) \quad (4)$$

Where, T_{af} is the air temperature with in the canopy, σ_f is the fractional vegetation coverage, T_a is the air temperature at the instrument height, T_f is the foliage temperature and T_g is the ground surface temperature.

$$W_{af} = 0.83 \sigma_f W \sqrt{C_{hnf}} + (1 - \sigma_f)W \quad (5)$$

Where, W_{af} is the wind speed with in the canopy, σ_f is the fractional vegetation coverage, W is the wind speed above the canopy and C_{hnf} is the near-neutral transfer coefficient al foliage layer [20].

$$C_{hnf} = K_v^2 \left(\ln \left(\frac{Z_a - Z_d}{Z_{o,f}} \right) \right)^{-2} \quad (6)$$

Where, C_{hnf} is the near-neutral transfer coefficient al foliage layer, K_v^2 is the von Karmen constant (0.4), Z_a is the instrument height, Z_d is the displacement height and $Z_{o,f}$ is the foliage roughness length scale.

Finally, the bulk transfer coefficient as defined by Deardorff is given by [19]:

$$C_f = 0.01 \times \left(1 + \frac{0.3}{W_{af}} \right) \quad (7)$$

Where, C_f is the bulk heat transfer coefficient and W_{af} is the wind speed with in the canopy.

Latent heat flux in the foliage layer

$$r_s = \frac{r_{s,min}}{LAI} f_1 f_2 f_3 \quad (8)$$

Where, r_s is the stomatal resistance, $r_{s,min}$ is the minimum stomatal resistance. The stomatal resistance at any time is proportional to this minimum resistance and inversely proportional to LAI. Stomatal resistance is modified by factors related to incoming solar radiation and atmospheric humidity. f_1 is the multiplying factor for the radiation effect on stomatal resistance, f_2 is the multiplying factor for the moisture effect on stomatal resistance and f_3 is the additional multiplying factor for stomatal resistance [22].

$$r_a = \frac{1}{C_f W_{af}} \quad (9)$$

Where, r_a is the resistance to moisture exchange offered by the boundary layer formed on the leaf surface, C_f is the bulk heat transfer coefficient and W_{af} is the wind speed with in the canopy.

$$r'' = \frac{r_a}{r_a + r_s} \quad (10)$$

Where, r'' is the foliage surface wetness factor, r_a is the resistance to moisture exchange and r_s is the stomatal resistance. From Henderdson-Sellers [21].

$$L_f = l_f LAI \rho_{af} C_f W_{af} r'' (q_{af} - q_{f,sat}) \quad (11)$$

Where, L_f is the foliage latent heat flux, l_f is the latent heat of vaporization at foliage temperature, LAI is the leaf area index, ρ_{af} is the density of air at foliage temperature, C_f is the bulk heat transfer coefficient, W_{af} is the wind speed with in the canopy, r'' is the foliage surface wetness factor, q_{af} mixing ratio for air within foliage canopy and $q_{f,sat}$ saturation mixing ratio at foliage temperature [16].

$$q_{af} = \frac{[(1 - \sigma_f)q_a + \sigma_f(0.3q_a + 0.6q_{f,sat}r'' + 0.1q_{g,sat}M_g)]}{1 - \sigma_f[0.6(1 - r'') + 0.1(1 - M_g)]} \quad (12)$$

Where, q_{af} is the mixing ratio for air within foliage canopy, σ_f is the fractional vegetation coverage, q_a is the mixing ratio for air, $q_{f,sat}$ is the saturation mixing ratio at foliage temperature, r'' is the foliage surface wetness factor, $q_{g,sat}$ is the saturation mixing ratio at ground temperature and M_g is the moisture saturation factor (0 to 1) is the ratio of volumetric moisture content to the porosity of the soil [16].

The latent heat of vaporization l_f is the amount of energy required to convert a unit mass of water to vapor.

$$l_f = 1.91846 \times 10^6 \left[\frac{T_f}{T_f - 33.91} \right]^2 \quad (13)$$

Where, l_f is the amount of energy required to convert a unit mass of water to vapor and T_f is the foliage temperature [21].

Soil energy budget.

$$F_g = (1 - \sigma_f)[I_s(1 - \alpha_g) + \varepsilon_g I_{ir} - \varepsilon_g \sigma T_g^4] - (T_g^4 - T_f^4) + H_g + L_g + K \times \frac{\partial T_g}{\partial z} \quad (14)$$

As with the energy equation for foliage, this equation accounts for sensible heat flux (H_g), latent heat flux (L_g) and the multiple reflections associated with long and short-wave radiation. The last term on the right represents the heat flux by conduction towards the soil substrate. Where, σ_f is the fractional vegetation coverage, I_s is the total incoming short-

wave radiation, α_g is the albedo (short-wave reflectivity) of ground surface, ε_g is the emissivity of ground surface, I_{ir} is the total incoming long-wave radiation, is the Stefan-Boltzmann constant ($5.67 \times 10^{-8} \text{ W/m}^2\text{K}^4$), T_g^4 is the ground surface temperature, T_f^4 is the foliage temperature, H_g is the ground sensible heat flux, L_g is the ground latent heat flux and z is the height or depth [16].

Sensible heat flux in the soil layer.

$$H_g = \rho_{ag} C_{p,a} C_{hg} W_{af} (T_{af} - T_g) \quad (15)$$

Where, H_g is the ground sensible heat flux, ρ_{ag} is the density of air at ground surface temperature, $C_{p,a}$ is the specific heat of air at constant pressure (1005.6 J/kg K), C_{hg} is the sensible heat flux bulk transfer coefficient at ground layer, W_{af} is the wind speed with in the canopy, T_{af} is the air temperature with in the canopy and T_g is the ground surface temperature [16].

$$\rho_{ag} = 0.5(\rho_a + \rho_g) \quad (16)$$

Where, ρ_{ag} is the density of air at ground surface temperature, ρ_a is the density of air at instrument height and ρ_g is the density of air at the ground surface temperature [16].

Linearized system of equations.

$$[T_f^{n+1}]^4 = [T_f^n]^4 + \alpha [T_f^n]^3 [T_f^{n+1} - T_f^n] \quad (17a)$$

$$[T_g^{n+1}]^4 = [T_g^n]^4 + \alpha [T_g^n]^3 [T_g^{n+1} - T_g^n] \quad (17b)$$

Where T_f^{n+1} and T_g^{n+1} are the current time step foliage and ground surface temperatures. T_f^n and T_g^n are the corresponding temperatures at the previous time step [19].

The saturation mixing ratios at the ground and foliage surface are given as:

$$q_{g,sat}(T_g^{n+1}) = q_{sat}(T_g^n) + \left(\frac{\partial q_{sat}}{\partial T} \right)_{T_g^n} (T_g^{n+1} - T_g^n) \quad (18a)$$

$$q_{f,sat}(T_f^{n+1}) = q_{sat}(T_f^n) + \left(\frac{\partial q_{sat}}{\partial T} \right)_{T_f^n} (T_f^{n+1} - T_f^n) \quad (18b)$$

where $q_{sat}(T_g^n)$ is the saturation mixing ratio at the previous time step and is formulated as given in Garrat [23]:

$$q_{sat}(T_g^n) = \frac{0.622e^*(T_g^n)}{P - e^*(T_g^n)} \quad (19)$$

Here the saturation vapor pressure e^* (Pa) is evaluated at the ground temperature from the previous time step (T_g^n) as:

$$e^* = 611.2 \exp \left[17.67 \left(\frac{T_g^n - 273.15}{T_g^n - 29.65} \right) \right] \quad (20)$$

The derivative of saturation mixing ratio at the previous time step is given by:

$$\frac{dq^*}{dT_g^n} = \left[\frac{0.622P}{(P - 0.378e^*)^2} \right] \left(\frac{de^*}{dT_g^n} \right) \quad (21)$$

Here, the derivative of the saturation vapor pressure can be calculated from the Clausius-Clapeyron equation [23]:

$$\frac{de^*}{dT_g^n} = \frac{l_g * P(T_g^n)}{(R_v * (T_g^n)^2)} \quad (22)$$

Where, R_v is the gas constant for water vapor and l_g is the latent heat of vaporization at the soil surface temperature.

The corresponding saturation mixing ratio relations for the leaf surfaces can be obtained by replacing T_g with T_f in the above relations.

Final equations.

After linearization the final equations are of the form:

$$C_{1,f} + C_{2,f}T_g + C_{3,f}T_f = 0 \quad (23a)$$

$$C_{1,g} + C_{2,g}T_g + C_{3,g}T_f = 0 \quad (23b)$$

The coefficients in these equations result from the direct combination of the previous development [16,17]. The coefficients involve the temperatures of the foliage and ground surface. This system of equations is solved simultaneously to obtain T_g and T_f . A key difference in the implementation of the FASST algorithm is that the conduction terms in the equations $C_{1,g}$ and $C_{2,g}$ are solved by inverting the conduction transfer functions (CFTs) within the solution implemented. The CFT analysis uses transient models of conduction through any material with thermal mass using the fixed space method. The general approach relates the heat flux at the surface of a building element to an infinite series of temperature histories at the boundary of both surfaces. The approximation of the infinite series is made by means of a finite series.

Software implementation

Inputs.

- Height of plants—the height of plants is limited to values in the range $0.01 < \text{height} < 1.0$ m.
- Leaf area index—the projected leaf area per unit area of soil surface. This field is dimensionless and is limited in this implementation to the range of $0.001 < \text{LAI} < 5.0$.
- Leaf reflectivity—the fraction of incident solar radiation reflected by the individual leaf surfaces. Solar radiation includes the visible spectrum as well as infrared and ultraviolet wavelengths.
- Leaf emissivity—the ratio of thermal radiation emitted from leaf surfaces to that emitted by an ideal black body at the same temperature. This parameter is used when calculating the long-wavelength radiant exchange at the leaf surfaces.
- Minimum stomatal resistance—the resistance of the plants to moisture transport in units of s/m. Plants with low values of stomatal resistance will result in higher evapotranspiration rates than plants with high resistance. Values for stomatal resistance are generally in the range of 50.0–300.0 s/m.
- Name of the soil layer—a unique reference name that the user assigns to the soil layer for a particular green roof.
- Roughness—a character string that defines the relative roughness of a particular material layer. This parameter only influences the exterior convection coefficient. A special keyword is expected in this field with the options being “VeryRough”, “Rough”, “MediumRough”, “MediumSmooth”, “Smooth”, and “VerySmooth”.
- Thickness—the depth of the growing media layer in meters.
- Conductivity—the thermal conductivity of the (dry) growing media in $W/(m\cdot K)$.
- Density—the density of the (dry) growing media in units of kg/m^3 .
- Specific heat—the specific heat of the (dry) growing media layer in units of $J/(kg\cdot K)$.
- Absorptance: thermal—the fraction of incident long wavelength radiation that is absorbed by the growing media.
- Absorptance: solar—the fraction of incident solar radiation that is absorbed by the (dry) growing media.
- Absorptance: visible—the fraction of incident visible wavelength radiation that is absorbed by the growing media.

3. Methodology

The process was divided into three parts, which were obtaining the data, validation of the model and experimentation with the variables to be studied.

A. Data collection

The research was carried out through the analysis of data previously obtained at the Autonomous University of Querétaro, where the implementation of a green roof system was carried out, as well as the installation of sensors to be able to collect the temperatures in the different layers of the system. Fig. 4 shows a scheme of the green roof system used and the areas where the readings were obtained [12].

The green roof is located in building H of the Graduate Department of the Faculty of Engineering on the Cerro de las Campanas Campus of the Autonomous University of Querétaro.

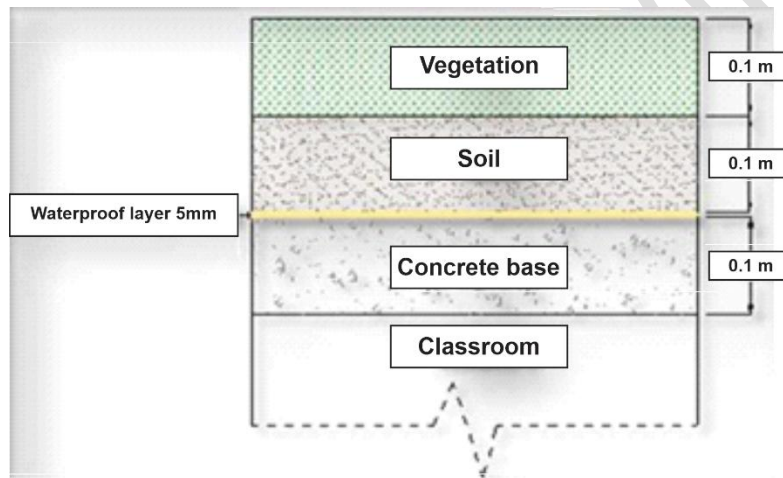


Figure 4 Section of the roof in a building of the Autonomous University of Queretaro

B. Model validation

Taking into account these data, the analysis of the general conditions of the model was carried out in order to verify the reliability of the model.

Ansys software [14], is a multiphysics simulation program for finite element analysis simulation, and the EnergyPlus engine [11], is capable of modeling buildings and verifying their energy consumption, either to increase the temperature or reduce it, ventilation and lighting. In addition, Open Studio [13], was used, as a series of tools that allow EnergyPlus to be used through a graphical interface [11], [23].

C. Experimentation of the study variables

Once the results were obtained, we proceeded to the variation of the input data with respect to the depth of the substrate layer and the change in climatic conditions by using a database corresponding to them for the place of study. With the results obtained from the previously conducted procedures, a comparison was obtained of the temperatures reached by the system using different substrate depth configurations for various times of the year.

4. Results and discussion

In Fig. 5 we can observe the comparison of the different internal temperatures obtained with each of the configurations, which start from a depth of 10 cm of substrate up to 30 cm with intervals of 5 cm, these obtained by means of EnergyPlus and Openstudio.

It can be seen that, in relation to the external and internal temperature with the green roof system, there is a difference of 5°C and in relation to the base classroom of 3°C with respect to the maximum temperature.

In Fig. 6 the data corresponding to the daily average for the whole year are presented, where the values obtained on the green roof with a 15 cm substrate, base room and external ambient temperature are compared. It was observed that the system helps to standardize the behavior of the internal temperature throughout the year, which prevents sudden changes in it regardless of the season.

In Figure 7a, we can observe the temperature distribution in the base classroom. This distribution was generated using the Ansys Mechanical APDL program. The model is configured to work with three-dimensional finite element elements, based on a one-dimensional transient analysis of heat transfer.

In Fig. 7b, the model is the same as the one in Fig. 7a, except for a layer of 15 cm of soil that was added on top of the external surface of the roof, simulating the effect of the green roof in terms of conduction, both figures have a scale from 18°C to 27.4°C, blue to red. We can observe in Figure 7b, in comparison with Figure 7a, that the temperature at the top corresponding to the roof is lower, and therefore its contribution to the increase in indoor temperature is reduced. We can also infer that the minimum temperature in the classroom is lower by observing the color distribution in both figures.

INDOOR AIR TEMPERATURE COMPARISON

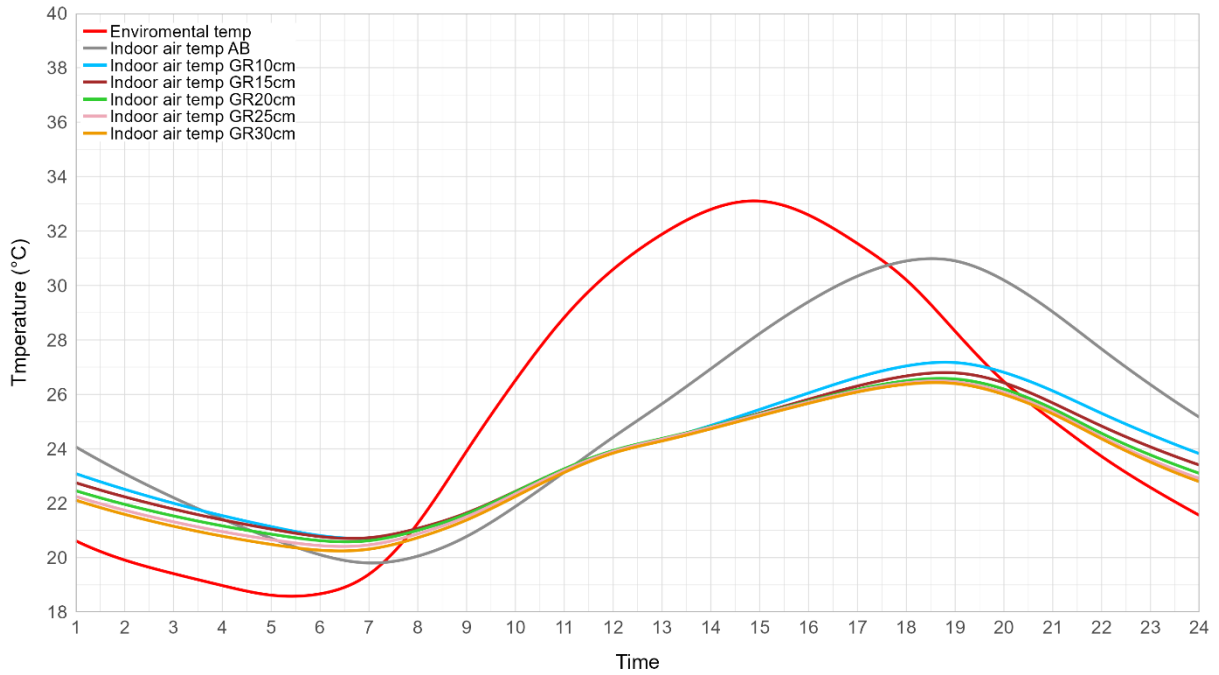


Figure 5 Internal temperatures of the green roof system with different substrate depths and the base model.

COMPARISON OF THE DAILY AVERAGE OF OUTDOOR AND INDOOR TEMPERATURES

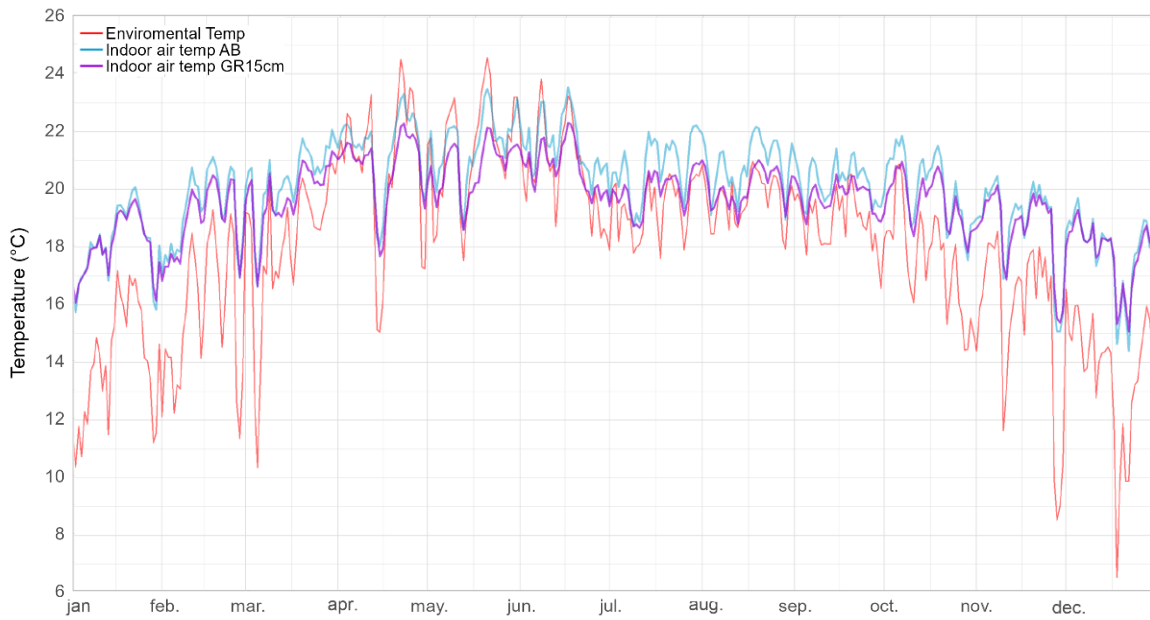


Figure 6 Daily average of internal temperature for green roof with 15 cm depth of substrate, base room and external temperature.

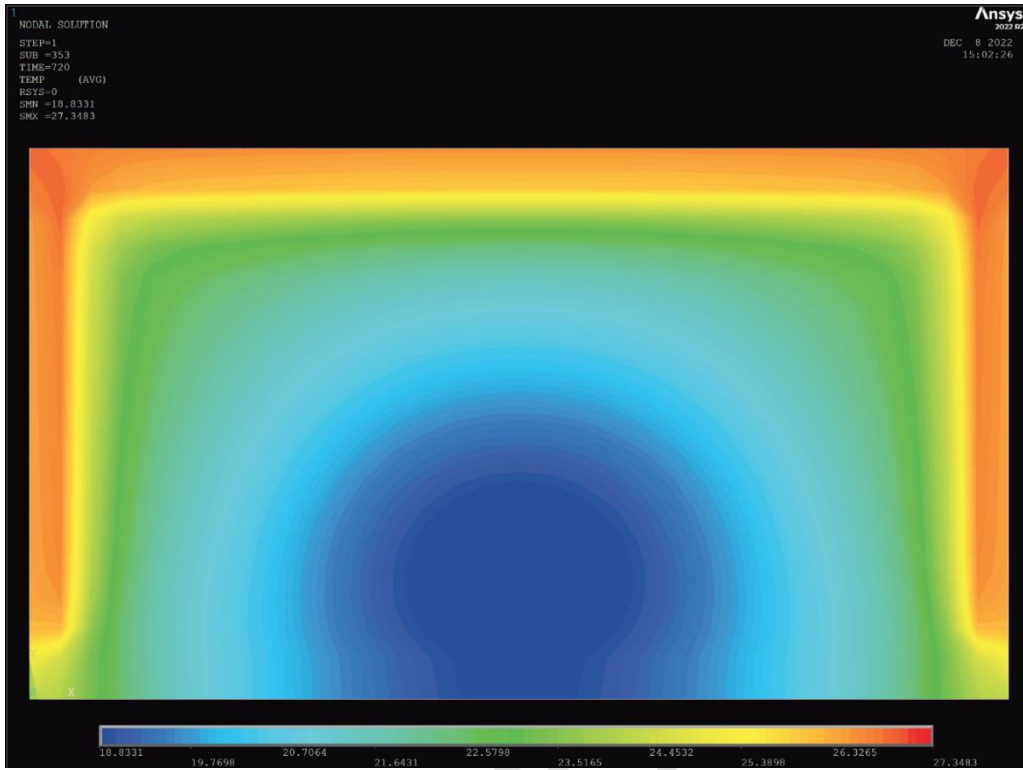


Figure 7 a) Distribution of internal temperatures(°C) in the base classroom. Scale from blue to red, from 18°C to 27.4°C.

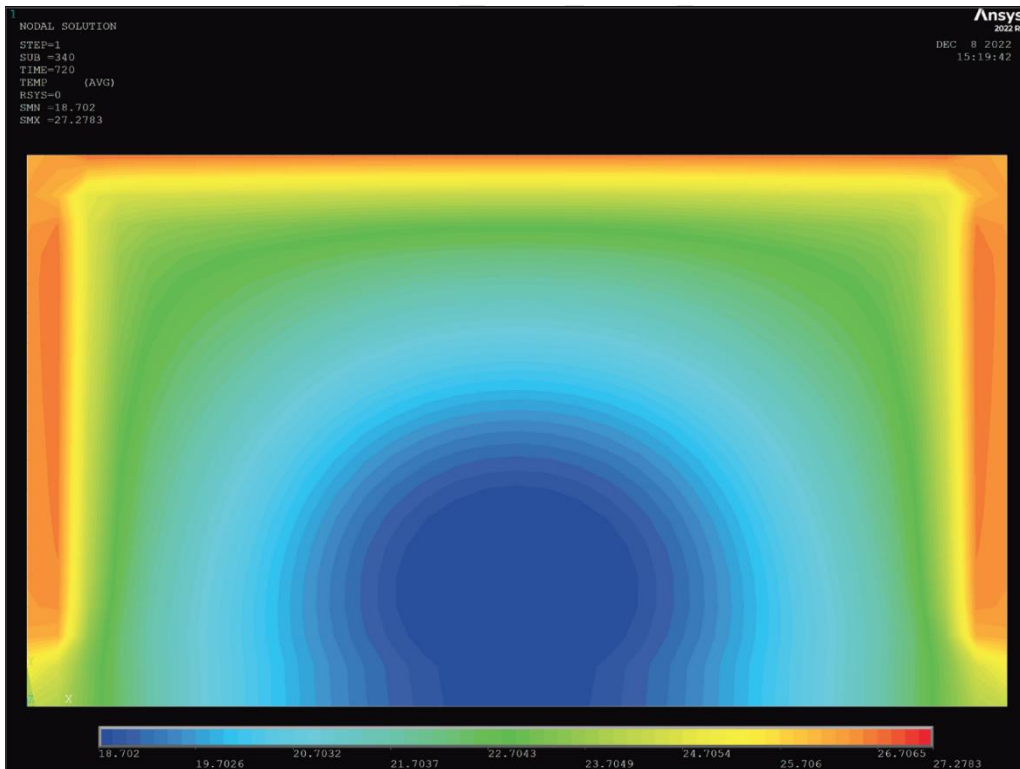


Figure 7 b) Distribution of internal temperatures(°C) in the classroom with a green roof with 15 cm depth of substrate. Scale from blue to red, from 18°C to 27.4°C.

5. Conclusion

With the results obtained from the different models, it was concluded that for the climate of Querétaro the optimum substrate thickness is 15 cm, which allows a decrease in internal temperature of 5°C.

This series of results also allowed us to reach the conclusion that for this type of climate it is not relatively important to have a substrate thickness greater than 15 cm, since the temperature differences between 15 and 30 cm are of 1°C In the case of extensive green lashes, which is the model that was worked with, this depth of substrate is adequate to meet the necessary conditions to sustain the life of the plants that will develop there.

Determining the thickness of 15 cm of substrate as appropriate for the type of climate also gives us the possibility of being able to implement it in a greater number of homes, since the weight of the systems in general will not represent as significant a load as a greater thickness.

References

- [1] G. Minke, Green Roofs. Planning, execution, practical advice. Artieda (Navarre). EcoHabitat., 2005.
- [2] N. Thuring, C. Dunnett, "Vegetation composition of old extensive green roofs.", Ecological Processes, 2014.
- [3] R. Sutton, Green Roof Ecosystems., vol. 23. London: Ed. Springer International Publishing, 2015.
- [4] Dunnett, N., and N. Kingsbury. Planting Green Roofs and Living Walls. Portland: Timber Press. 2004.
- [5] Castleton, HF, V. Stovin, SBM Beck, and JB Davison. "Green Roofs: Building Energy Savings and the Potential for Retrofit".Energy and Buildings 42 (10): 1582–1591.
- [6] National Energy Balance. Secretary of Energy. SENER. 2019.
- [7] Getter, K. Rowe, B. The role of extensive green roofs in sustainable development. 41. 2006.
- [8] Wong, NH, Cheong, DKW, Yan, H., Soh, J., Ong CL, Sia, A., 2003, The effects of rooftop garden on energy consumption of a commercial building in Singapore, Energy and Buildings, 35, pp. 353-364.

- [9] Kohler M, Schmidt M, Grimme FH, Laar M, Paiva VLA, Tavares S (2002) Green roofs in temperate climates and in the hot-humid tropics—far beyond the aesthetics. *environment manager Health* 13(4):382–391 doi:10.1108/09566160210439297.
- [10] Rowe DB, Monterusso MA, Rugh CL (2006) Assessment of heat-expanded slate and fertility requirements in green roof substrates. *Horttechnology* 16:471 – 477
- [11] EnergyPlus. EnergyPlus Documentation, Energy Simulation Software, version 9.5.0. united states Department of Energy. 2021.
- [12] Perez Gonzalez, MML (2010). Evaluation of thermal comfort and hydrological behavior in urban buildings with green roofs for semi-arid regions.
- [13] OpenStudio. OpenStudio Coalition Documentation, version 1.4.0. Alliance for Sustainable Energy, LLC. 2022.
- [14] Ansys Inc. Software 2022. Mechanical APDL Release Notes. Pittsburg, USA.
- [15] D.J. Sailor, A green roof model for building energy simulation programs, *Energy and Buildings*, Volume 40, Issue 8, 2008, Pages 1466-1478, ISSN 0378-7788, <https://doi.org/10.1016/j.enbuild.2008.02.001>.
- [16] S. Frankenstein, G. Koenig, FASST Vegetation Models, U.S. Army Engineer Research and Development Center, Cold Regions Research and Engineering Laboratory (ERDC/CRREL), Technical Report TR-04-25, 2004.
- [17] S. Frankenstein, G. Koenig, Fast all-season soil strength (FASST), U.S. Army Engineer Research and Development Center, Cold Regions Research and Engineering Laboratory (ERDC/CRREL), Special Report SR-04-01, 2004.
- [18] T.R. Oke, *Boundary Layer Climates*, Methuen, London, 1978, ISBN 0-416-04422-0.
- [19] J.W. Deardorff, Efficient prediction of ground surface temperature and moisture, with inclusion of a layer of vegetation, *Journal of Geophysical Research* 83 (1978) 1889–1903.
- [20] J.P. Hughes, D.P. Lettenmaier, Guttorp, A stochastic approach for assessing the effect of changes in regional circulation patterns on local precipitation, *Water Resources Research* 29 (1993) 3303–3315.
- [21] B. Henderson-Sellers, A new formula for latent heat of vaporization of water as a function of temperature, *Quarterly Journal of Royal Meteorological Society* 110. (1984) 1186–1190.
- [22] G.G. Koenig, Smart Weapons Operability Enhancement (SWOE) Joint Test and Evaluation (JTand E) Program: Final Report, Dr. James P. Welch, Joint Test Director, SWOE JT and E, SWOE Report 94-10, Annex D, 1994.

- [23] J.R. Garratt, The Atmospheric Boundary Layer, Cambridge University Press, 1992.
- Varzandeh A, Sajadi B. Energy performance sensitivity analysis on building's passive technologies effective parameters, in an NZEB EnergyPlus-simulated villa in Tehran's weather conditions with OFAT methods. Energy Equipment and Systems. 2023 Jun 1;11(2):213-29.

UNDER PEER REVIEW